

# Characterization of Poly(vinyl pyrrolidone-co-isobutylstyryl polyhedral oligomeric silsesquioxane) Nanocomposites

Hongyao Xu,<sup>1,2</sup> Shiao-Wei Kuo,<sup>1</sup> Chih-Feng Huang,<sup>1</sup> Feng-Chih Chang<sup>1</sup>

<sup>1</sup>Department of Applied Chemistry, National Chiao-Tung University, Hsin Chu, Taiwan, Republic of China

<sup>2</sup>Department of Chemistry, Anhui University, Anhui, 230039, China

Received 15 October 2002; accepted 22 July 2003

**ABSTRACT:** Poly(vinyl pyrrolidone-co-isobutyl styryl polyhedral oligomeric silsesquioxane)s (PVP-POSS) were synthesized by one-step polymerization and characterized using FTIR, high-resolution <sup>1</sup>H-NMR, solid-state <sup>13</sup>C-NMR, <sup>29</sup>Si-NMR, GPC, and DSC. The POSS content can be controlled by varying the POSS feed ratio. The  $T_g$  of the PVP-POSS hybrid is influenced by three main factors: (1) a diluent role of the POSS in reducing the self-association of the PVP; (2) a strong interaction between the POSS siloxane and

the PVP carbonyl, and (3) physical aggregation of nanosized POSS. At a relatively low POSS content, the role as diluent dominates, resulting in a decrease in  $T_g$ . At a relatively high POSS content, the last two factors dominate and result in  $T_g$  increase of the PVP-POSS hybrid. © 2003 Wiley Periodicals, Inc. *J Appl Polym Sci* 91: 2208–2215, 2004

**Key words:** glass transition; hybrid materials; nanocomposites; poly(vinylpyrrolidone); polysiloxanes

## INTRODUCTION

Synthetic polymers have played an increasingly important role in daily life because of their favorable processability and lower cost than those of other materials such as metals or ceramics. However, pure polymeric materials frequently face application limitations because of their low modulus and low thermal stability. An important approach to overcome these drawbacks is to develop new plastics that possess properties between those of an organic system (e.g., polymers) and a traditional inorganic system (e.g., ceramics). This concomitant effect creates a new field of hybrid materials. Typical hybrid materials contain three-dimensional crosslinked sol-gel networks, in which an inorganic silica-like phase is dispersed within the polymer matrix. Recently, well-defined polyhedral oligomeric silsesquioxane-based hybrid polymers have attracted increasing scientific interest.<sup>1</sup> Several nanocomposite hybrid polymers have been prepared from polyhedral oligomeric silsesquioxanes (POSS)<sup>2–15</sup> and exhibit increased  $T_g$ ,<sup>2–4,15</sup>  $T_{dec}$ ,<sup>5</sup> resistance to oxidation,<sup>6</sup> and miscibility as well as reduced flammability. The POSS is a cubic silica that is rigid

and has completely defined dimension (0.53 nm) with eight organic groups (functional or inert) appended to the vertices of the cube. The functional groups can be selectively varied to prepare various POSS-based hybrid polymers. For example, a single-functional POSS is used to prepared pendant-type hybrid polymers, a double-functional POSS is used to prepare backbone-type polymers, and the multifunctional POSS is suitable for the crosslinking-type hybrid polymers.

In this work, copolymers from vinyl pyrrolidone and isobutylstyryl polyhedral oligomeric silsesquioxanes and their molecular structures were characterized using high-resolution NMR, FTIR, DSC, and GPC.

## EXPERIMENTAL

### Materials

Isobutyl styryl polyhedral oligosilsesquioxane (POSS) was purchased from the Hybrid Plastic Co. and kept in a dried box before use. Vinylpyrrolidone (VP) was purchased from Aldrich (Milwaukee, WI), distilled from calcium hydride under reduced pressure, and stored in sealed ampoules in a refrigerator. High-purity azobisisobutyronitrile (AIBN), also from Aldrich, was kept in a dried box and used as received. Spectroscopic-grade THF and toluene were dried over 4-Å molecular sieves and distilled from sodium benzophenone ketyl immediately before use. All other solvents were purchased from Aldrich and used without further purification.

Correspondence to: F.-C. Chang (changfc@cc.nctu.edu.tw).  
Contract grant sponsor: National Science Council, Taiwan; contract grant number: NCS-90-2216-E-009-016.  
Contract grant sponsor: National Natural Science Fund of China; contract grant number: 50073001.

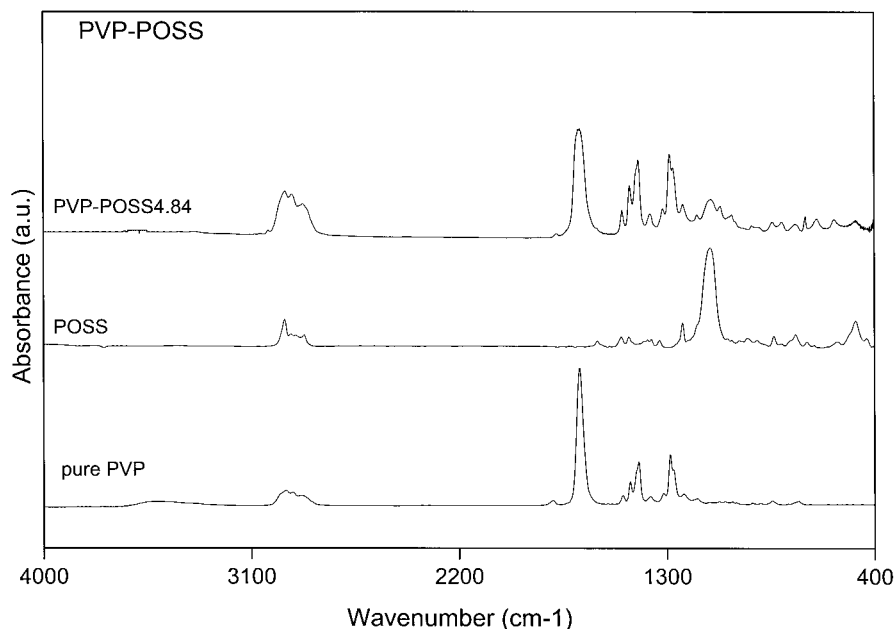


**Figure 1** FTIR spectra in the region of 4000–400  $\text{cm}^{-1}$ , recorded at room temperature, of pure POSS, parent PVP, and PVP-POSS4.84.

### Preparation of samples

All polymerization reactions were carried out under nitrogen using a vacuum-line system. These poly(vinylpyrrolidone-*co*-isobutylstyrylPOSS)s (PVP-POSS) copolymers were prepared by a free-radical polymerization method. For comparison, a pure poly(vinylpyrrolidone) (PVP) was also synthesized. A typical example of experimental procedure to synthesize these polymers is given below. In a typical reaction, 9.8 mmol of VP and 0.22 mmol of POSS monomer in 10 mL dried toluene were polymerized using an AIBN initiator (1 wt % based on monomer) at 80°C under nitrogen atmosphere for 24 h. The product then was poured into excess cyclohexane under vigorous stirring to precipitate the copolymer, then purified in THF/cyclohexane and dried in a vacuum oven. A 58.4% product yield was obtained through this procedure.

### Instrumentation analyses

Thermal analyses were performed on a DSC from Dupont (DSC-9000; Dupont, Boston, MA). The scan rate was 20°C/min within the temperature range of 30–260°C. The sample was quickly cooled to 0°C from the melt for the first scan and then scanned from 20 to 280°C at 20°C/min. The glass-transition temperature ( $T_g$ ) was taken as the midpoint of the specific heat increment. FTIR spectra were measured with a spectral resolution of 1  $\text{cm}^{-1}$  on a Nicolet Avatar 320 FTIR spectrophotometer (Nicolet Analytical Instruments, Madison, WI) using KBr disks or film at room temper-

ature. Weight-average ( $M_w$ ) and number-average ( $M_n$ ) molecular weights and polydispersity index (PDI,  $M_w/M_n$ ) were determined by a Waters 510 gel permeation chromatograph (GPC; Waters Chromatography Division/Millipore, Milford, MA).  $^1\text{H-NMR}$  spectra were recorded on a Bruker ARX300 spectrometer (Bruker Instruments, Billerica, MA) using chloroform-*d* solvent. High-resolution solid-state  $^{13}\text{C-NMR}$  and  $^{29}\text{Si-NMR}$  experiments were carried out at room temperature using a Bruker DSX-400 spectrometer operating at resonance frequencies of 100.46 and 79.38 MHz, respectively. The CP/MAS spectra were measured with a 3.9- $\mu\text{s}$  90° pulse, with 3-s pulse delay time, acquisition time of 30 ms, and 2048 scans. All NMR spectra were taken at 300 K using broad band proton decoupling and a normal cross-polarization pulse sequence. A magic angle sample spinning (MAS) rate of 5.4 kHz was used to avoid absorption overlapping.

## RESULTS AND DISCUSSION

Relevant synthesis and polymerization dynamics were previously documented elsewhere.<sup>4</sup> Figure 1 shows the FTIR spectra of PVP-POSS, pure POSS, and pure PVP. The pure POSS exhibits a characteristically symmetric Si—O—Si stretching absorption band at 1109  $\text{cm}^{-1}$  and an aromatic  $\nu_s$  —(C—H) stretching vibration at 3000–3100  $\text{cm}^{-1}$ . PVP shows the characteristic carbonyl vibration absorption at 1680  $\text{cm}^{-1}$ , strong  $\nu_s$  (O=C—N) stretching at 1490  $\text{cm}^{-1}$ , and strong  $\nu_s$  ( $\text{CH}_2$ —C—N in pyrrolidonyl ring) stretching at 1350

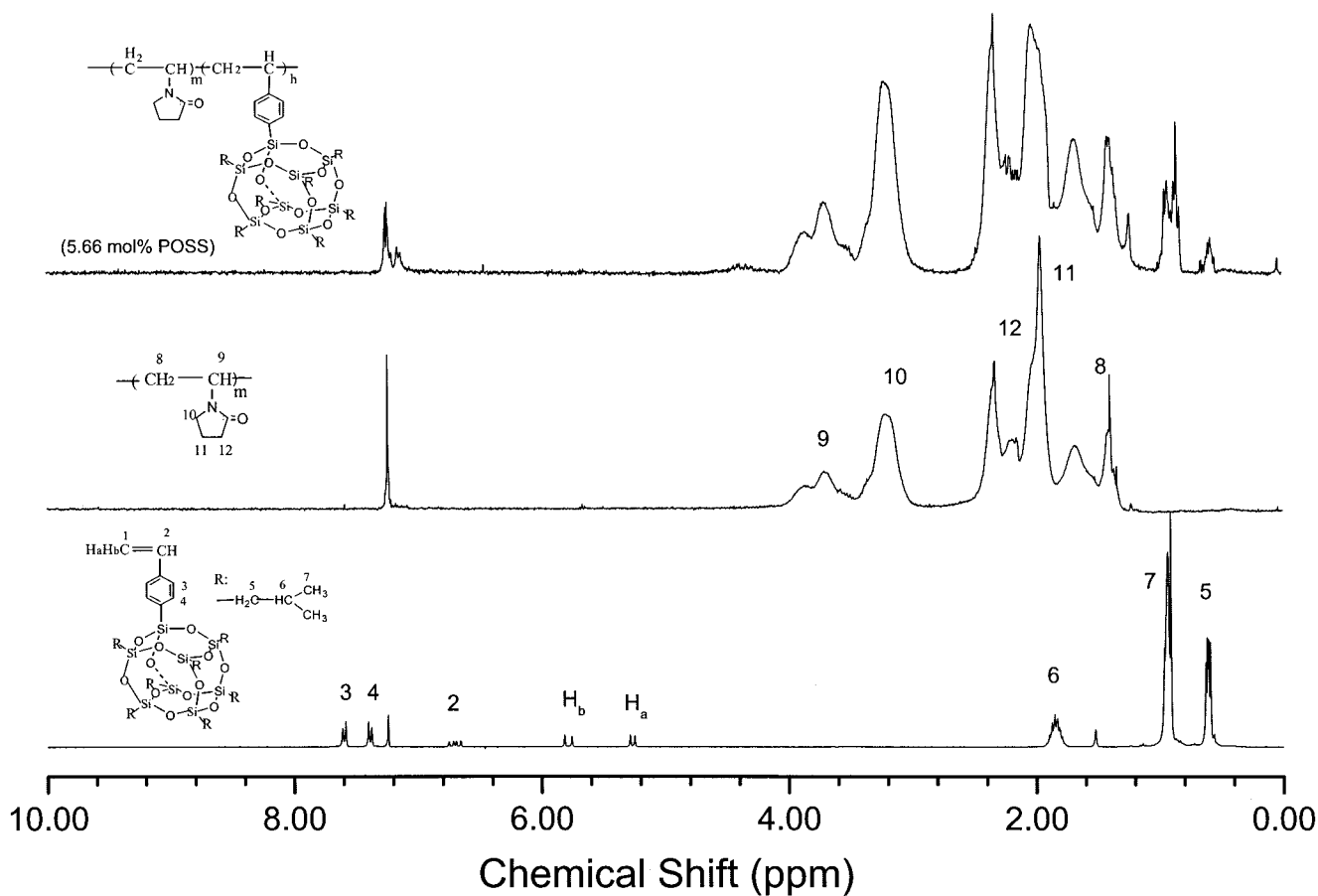


**Figure 2**  $^1\text{H-NMR}$  spectra of the pure POSS, parent PVP, and PVP-POSS4.84.

$\text{cm}^{-1}$ . The spectrum for PVP-POSS is almost identical to that for the PVP except for a sharp, strong, and symmetric Si—O—Si stretching peak [ $\nu_s$  (Si—O—Si)] at about  $1109\text{ cm}^{-1}$  from the silsesquioxane cages.<sup>16,17</sup> The consistent presence of this characteristic peak ( $\sim 1109\text{ cm}^{-1}$ ) confirms that the POSS cube structure is present in the formed hybrid copolymer. The intensity of this characteristic Si—O—Si absorption band in the copolymer increases with the POSS feed ratio. Compared with that of the PVP, the PVP-POSS shows a new weak aromatic  $\nu_s$  (C—H) absorption at  $3000\text{--}3100\text{ cm}^{-1}$ , which is assigned as the substituted aromatic group in POSS.

The PVP-POSS hybrid copolymer is soluble in most organic solvents: its structure can therefore be characterized by using the NMR spectra. Figure 2 shows  $^1\text{H-NMR}$  spectra of pure POSS, PVP, and PVP-POSS containing 5.66 mol % of POSS in *d*-chloroform solvent. For the pure POSS macromer, proton resonance absorptions of methyl (7), methylene (5), and methane (6) proton resonance absorption from the substituted isobutyl group at the mole ratio of 3 : 2 : 1 are located at  $\delta$  0.92, 0.60, and 1.85 ppm, respectively. A doublet and a quartet resonance proton resonance peak ( $1\text{H}_a$ ,  $1\text{H}_b$ , and 2) from the vinyl group in the POSS are

located at 5.26, 5.77, and 6.98 ppm with a relative mole ratio of 1 : 1 : 1, corresponding to *iso*-, *trans*-, and *substituted* vinyl proton peaks, respectively. However, these characteristic peaks disappear after polymerization with vinyl pyrrolidone, indicating the total consumption of the POSS. The doublet aromatic proton peaks, for a relative mole ratio of 1 : 1, are present at 7.38 and 7.59 ppm, respectively. These peaks shift to a higher field after copolymerization with *N*-vinyl pyrrolidone to form the PVP-POSS copolymer, further confirming that the POSS is indeed incorporated into PVP. In pure PVP, the methine proton (9) peak in the backbone is at  $\delta$  3.70 ppm, which overlaps with the methine proton peak in the backbone from the POSS segment in the PVP-POSS copolymer. The resonance observed at  $\delta$  3.19 ppm is assigned to the methylene protons (10) adjacent to the nitrogen atom in the pyrrolidonyl ring. The methylene proton (8) in the backbone overlaps with the methylene protons (11,12) from the pyrrolidonyl ring, as shown at  $\delta$  1.30–1.85 and  $\delta$  1.85–2.70 ppm (Fig. 2). In the PVP-POSS copolymer, essentially all PVP characteristic resonances are clearly present in the spectra of the copolymers. The resonant proton peak at  $\delta$  1.30–2.70 ppm is relatively enhanced compared with that of the pure PVP, attrib-

TABLE I  
Summary of POSS Content, Thermal Properties, and GPC Data of Various PVP-POSS

Sample	POSS <sup>a</sup> (mol %)	POSS <sup>b</sup> (mol %)	$T_g^c$ (°C)	$M_w^d$ ( $\times 10^3$ g/mol)	$M_n$ ( $\times 10^3$ g/mol)	PDI <sup>e</sup>
1	0.00	0.00	149.52	599.8	131.6	4.56
2	2.00	1.68	138.90	166.9	142.5	1.17
2	3.01	2.75	155.72	177.8	148.5	1.20
3	5.14	4.84	167.97	126.7	111.8	1.13
4	7.73	5.66	171.94	208.8	184.1	1.13
5	11.62	9.43	178.32	161.1	143.8	1.12

<sup>a</sup> Data were obtained based on IR standard curve.<sup>6</sup>

<sup>b</sup> Determined by <sup>1</sup>H-NMR.

<sup>c</sup> Data were gathered on the second melt using a heating and cooling rate of 20°C/min.

<sup>d</sup> Determined by GPC using PS standard curve.

<sup>e</sup> PDI, polydispersity index ( $M_w/M_n$ ).

uted to the overlap with the resonance of the methylene and methine protons in the backbone from the POSS segment of the PVP-POSS.

The <sup>1</sup>H-NMR spectra from all copolymers clearly show the methyl protons and the methylene protons from the isobutyl group of the POSS moiety. However, the vinyl protons from POSS completely disappear and these aromatic proton peaks shift to a higher field at  $\delta$  7.06–7.18 ppm, further verifying that the POSS has copolymerized with vinylpyrrolidone. The ratio of PVP to POSS is estimated by directly comparing the peak area of the methylene proton (10) adjacent to nitrogen in the pyrrolidonyl ring in the PVP segment ( $\delta$  3.20 ppm) to the peak area of methyl (7) protons from isobutyl of the POSS segment ( $\delta$  = 0.92 ppm). The POSS contents in various PVP-POSS copolymers are summarized in Table I.

High-resolution solid-state <sup>13</sup>C-NMR spectroscopy provides further insight into the copolymerization of the vinyl pyrrolidone and the POSS macromer. Figure 3 shows the high-resolution solid-state <sup>13</sup>C-NMR spectra of various PVP-POSS copolymers, pure PVP, and the pure POSS. Pure POSS shows three strong resonance peaks at 24.4 (C-7), 26.7 (C-5), and 27.6 (C-6) ppm, associated with the isobutyl group of POSS macromer, and six weak resonance peaks in the low field at 114.2, 125.9, 130.7, 134.4, 137.5, and 139.7, corresponding to the styryl group of POSS. PVP also shows six resonance peaks at 176.8, 43.8, 38.2, 32.0, and 19.1 ppm, in which the C-9 and C-10 resonance peaks from the pyrrolidonyl ring overlap and give a peak maximum at 43.8 ppm. The resonance peak at 176.8 ppm comes from the carbonyl carbon (C-13). All other resonance peak assignments are given in Figure 3.

<sup>13</sup>C-NMR spectra from all PVP-POSS copolymers clearly show these PVP resonance peaks. In comparing with that of the PVP, strong resonance absorptions from 20.0 to 30.0 ppm are observed in all PVP-POSS hybrids, which correspond to the isobutyl group of the POSS. In addition, the intensities of these resonances increase with the increase of POSS content. These res-

onance peaks can be clearly observed when the POSS content is greater than 4.84 mol %, further confirming that the POSS moiety is indeed incorporated into the PVP. The <sup>29</sup>Si-NMR spectra of various PVP-POSS hybrids were also measured to further confirm the incorporation of POSS moieties into PVP. Figure 4 shows expanded <sup>29</sup>Si-NMR spectra of pure POSS and a typical PVP-POSS hybrid (5.66 mol % POSS). The pure POSS shows two characteristic silica resonance bands at -67.8 and -79.9 ppm, corresponding to the silicas in the POSS core substituted by isobutyl group and styryl group, respectively. The two characteristic resonances also appear in all PVP-POSS hybrids, providing additional evidence that the POSS moiety is attached to the PVP.

Figure 5 shows the expanded carbonyl carbon resonance spectra of the pure PVP and various PVP-POSS hybrids in the region of 182–172 ppm. Interestingly, the maximum peak positions of carbonyl carbon resonances of these PVP-POSS copolymers vary as the POSS is added, as shown in Figure 5. The carbonyl carbon resonance peak of pure PVP (176.8 ppm) shifts significantly to a higher field at a relatively low POSS content when the POSS moiety is incorporated into the PVP. It is well known that the chemical and physical environmental variations of a molecule will cause a chemical shift. The shift phenomenon is also found in our other POSS-based hybrid systems. The POSS, when incorporated into the PVP, mainly acts as an inert diluent to the carbonyl-carbonyl dipole-dipole self-association interaction and causes the carbonyl carbon resonance to shift toward a higher field. For example, the PVP-POSS1.68 shows a high field shift of 1.1 ppm compared with that of the pure PVP attributed to the diluent effect of the POSS on the self-association interaction of the carbonyl group in the PVP. This chemical shift further increases with the increase of the POSS content (PVP-POSS2.75) initially. However, the resonance peak does not shift to a higher field when the POSS content is further increased. On the contrary, it shifts slightly downfield

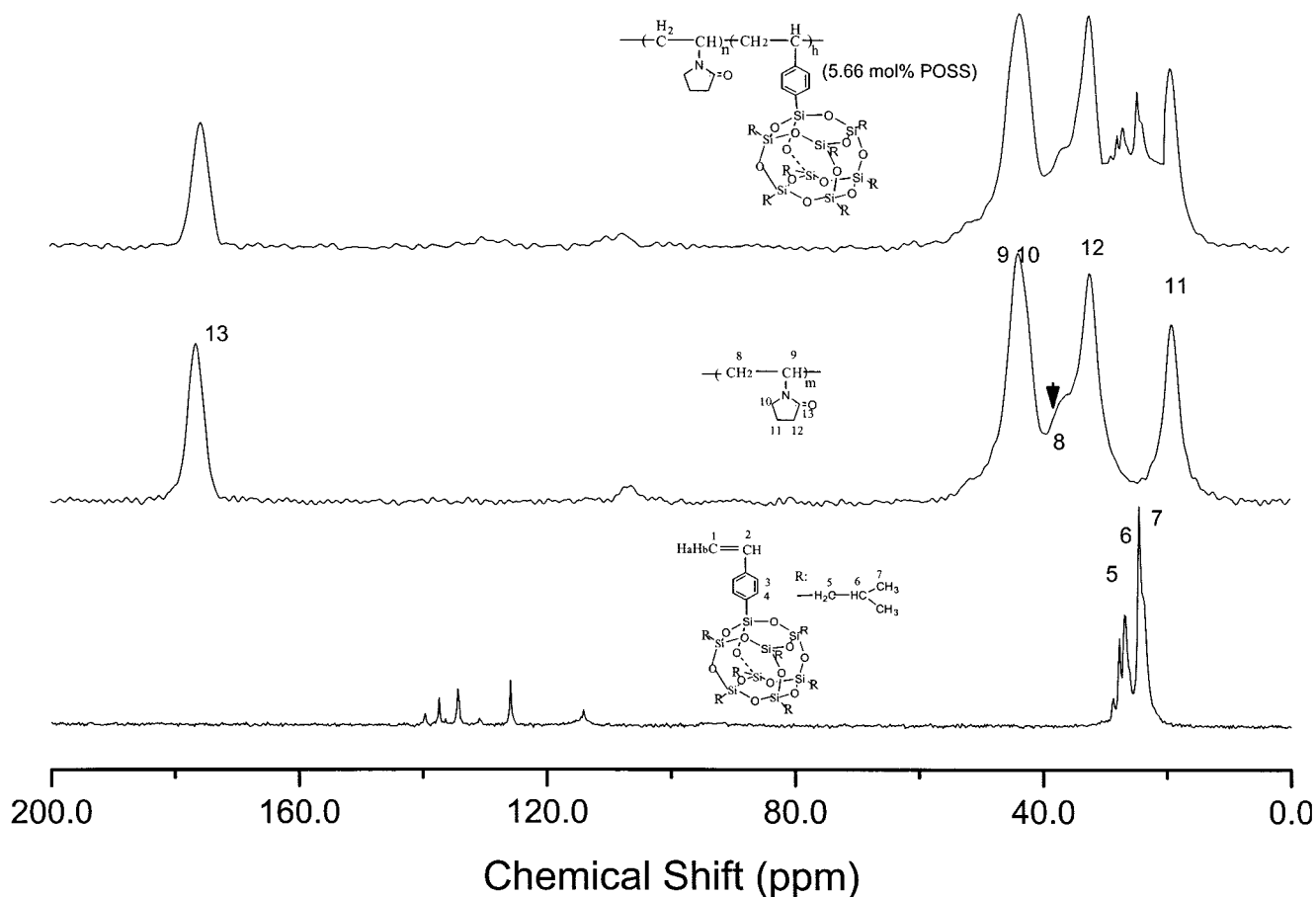


**Figure 3** High-resolution solid-state  $^{13}\text{C}$ -NMR spectra of the pure POSS, parent PVP, and PVP-POSS5.66.

compared with that of PVP-POSS2.75. For example, PVP-POSS2.75 shows a shift of 1.5 ppm, whereas the PVP-POSS9.43 has a shift of only 1.0 ppm, implying that a new interaction occurs between the POSS and the PVP besides the diluent effect of the POSS. At a relatively low POSS content, the POSS mainly plays an inert diluent role to the carbonyl group self-associated interaction. At a relatively high POSS content, the strong dipole-dipole interaction between siloxane of POSS and carbonyl group of PVP becomes dominant and thus reduces its high-field shift of the carbonyl carbon resonance as a result of the diluent effect from the POSS.

Figure 6 plots the resulting  $T_g$  and the chemical shift of the carbonyl carbon versus the POSS mole fraction in PVP-POSS. Quite unexpectedly, when a small amount of the POSS is incorporated into the PVP to produce the PVP-POSS hybrid (PVP-POSS1.68), its  $T_g$  (138.9°C) actually decreases from that of the parent PVP (149.5°C) by about 10°C. However, when higher POSS content is incorporated into the PVP (PVP-POSS2.85), its  $T_g$  (155.7°C) becomes 6°C higher than that of the parent PVP. As shown in Table I, when the POSS content exceeds 3 mol %, the  $T_g$  of PVP-POSS increases with the increase of the POSS content. For

instance, PVP-POSS4.84 has a  $T_g$  of 167.9°C, which is 18°C higher than that of the parent PVP. Similar results were obtained in other POSS-based hybrids by Lichtenhan.<sup>2,3</sup>

In the  $^{29}\text{Si}$ -NMR spectra (Fig. 4), the characteristic band at  $-67.8$  ppm also shifts downfield when POSS is incorporated into the PVP. For example, the resonance maximum of the PVP-POSS1.68 ( $-67.4$  ppm) shifts downfield by about 0.4 ppm from the pure POSS. This observed downfield shift indicates that the POSS interacts with PVP and further supports the previously published mechanism of increasing  $T_g$  of the POSS-based hybrid.<sup>4</sup> The POSS resonance at  $-67.8$  ppm always shifts downfield after being incorporated into PVP. However, the characteristic resonance of the PVP-POSS hybrid shifts toward the high field as the POSS content is further increased. This phenomenon possibly can be interpreted as being attributed to POSS aggregation. Figure 7 shows the effect of POSS content on chemical shift of  $^{29}\text{Si}$ -NMR. For example, the characteristic resonance of the PVP-POSS is a broad symmetric peak at a low POSS content and becomes a steep and sharp peak at a higher POSS content (PVP-POSS9.34), which is similar to that of pure POSS. Figure 8 shows the relationship between

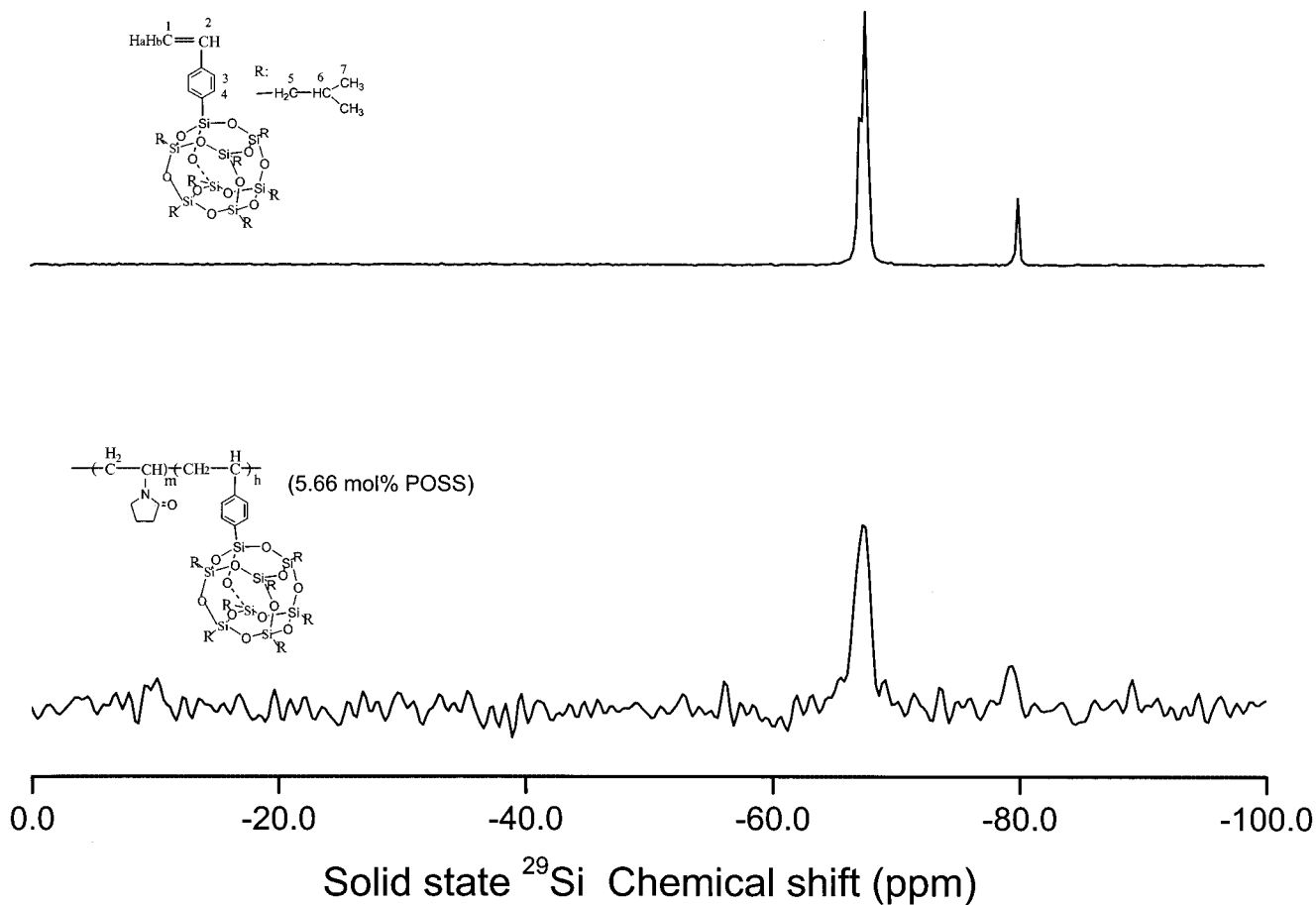


Figure 4 High-resolution solid-state  $^{29}\text{Si}$ -NMR spectra of the pure POSS and the PVP-POSS5.66.

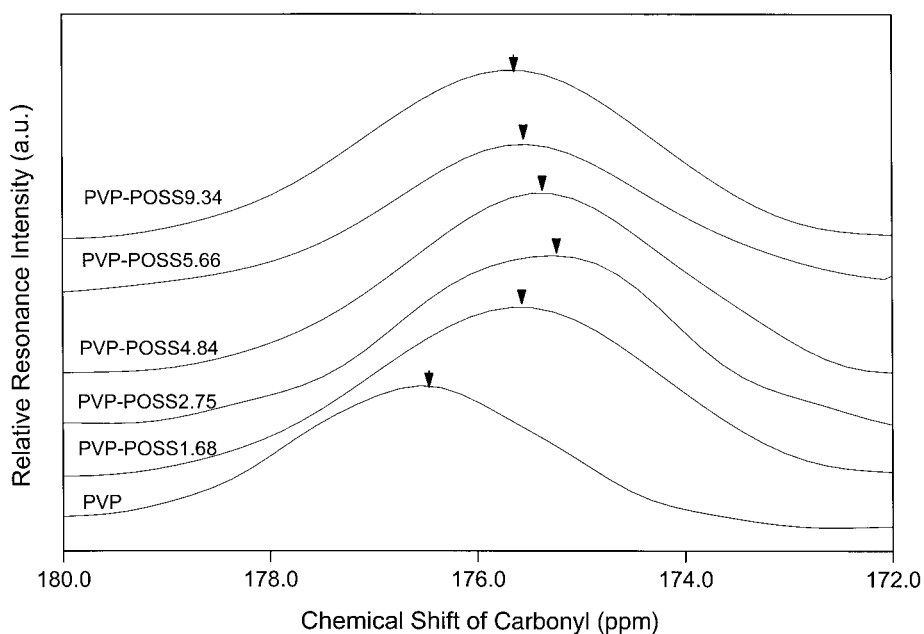
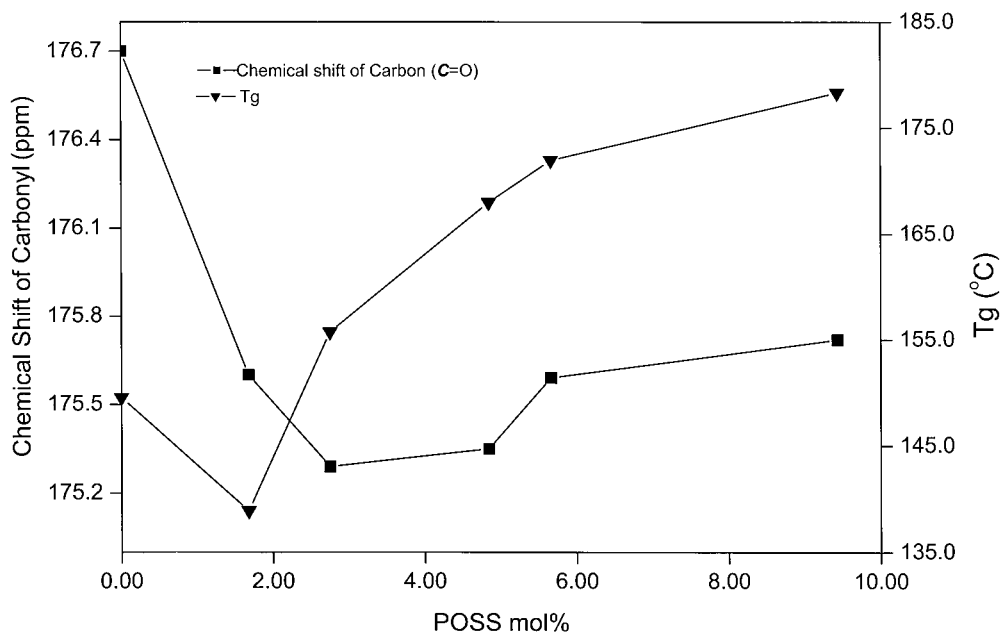


Figure 5 Expanded solid-state  $^{13}\text{C}$ -NMR spectra of the pure POSS, parent PVP, and PVP-POSS4.84 in the regions 182.0–172.0 ppm.



**Figure 6** Relationship of the chemical shift of the carbonyl carbon resonance and the POSS fraction in the hybrids.

the chemical shift of  $^{29}\text{Si}$  resonance and the POSS mole fraction of various PVP-POSS copolymers. The relationship between  $T_g$  and POSS content of PVP-POSS hybrids is also shown for comparison. The  $T_g$  of the PVP-POSS hybrid decreases at low POSS content because of the diluent effect of the POSS to reduce the self-association of PVP. The increase in  $T_g$  of the PVP-POSS hybrid at a high POSS content comes from the increased interaction between the siloxane of POSS

and the dipole carbonyl group of PVP, as well as the nanoscale POSS physical aggregation.

## CONCLUSIONS

The well-defined nanoscale isobutyl styryl polyhedral oligomeric silsesquioxane (POSS) was incorporated into the poly(vinylpyrrolidone) by simple free-radical polymerization. The POSS content in the PVP-POSS

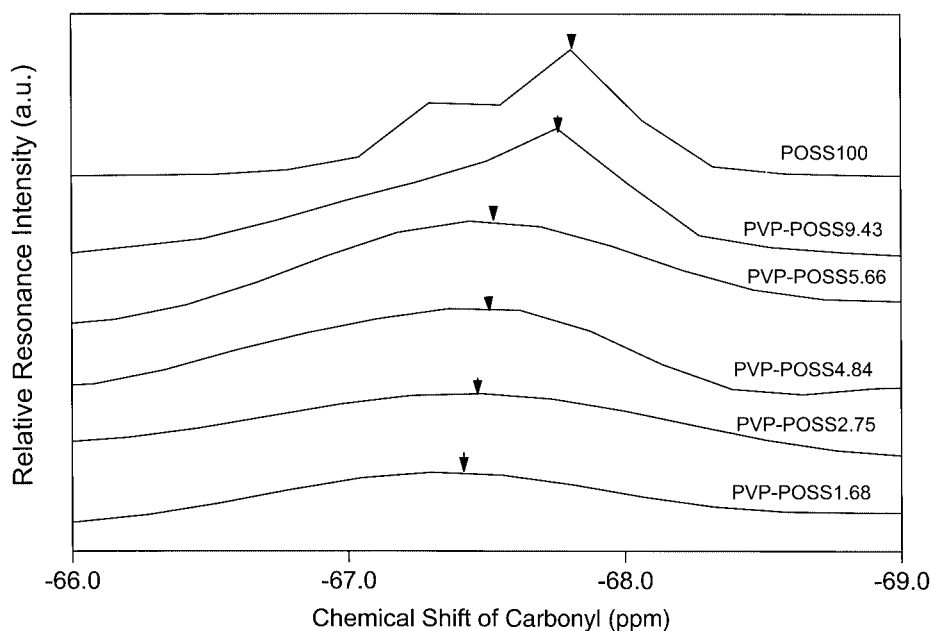


**Figure 7** Expanded solid-state  $^{29}\text{Si}$ -NMR spectra of the pure POSS and various PVP-POSS hybrids from  $-66.0$  to  $-69.0$  ppm.

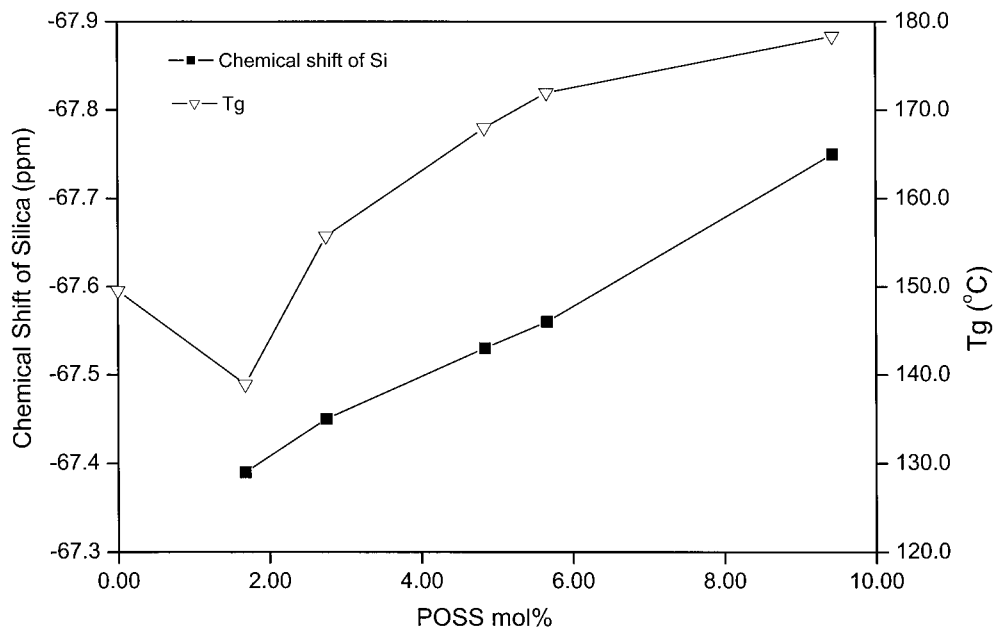


**Figure 8** Relationship between the  $T_g$ , the chemical shift of silica, and the POSS fraction in the hybrid.

hybrid can be varied by changing the POSS feed ratio. The microstructure of the PVP-POSS hybrid nanocomposite was characterized by high-resolution NMR spectra and FTIR. The  $T_g$  value of the PVP-POSS hybrid decreases at a low POSS content because POSS acts as a diluent to reduce the self-association interaction of PVP. The  $T_g$  of PVP-POSS increases at a high POSS content. High-resolution NMR and FTIR spectra provide important information on the proposed  $T_g$  enhancement mechanism. At a higher POSS content, the interaction between the siloxane of POSS and the dipole carbonyl group of PVP, as well as the physical aggregation of nanoscale POSS, result in an increase in  $T_g$  of the PVP-POSS hybrid.

This work was financially supported by the National Science Council, Taiwan, under contract number NCS-90-2216-E-009-016 and supported in part by the National Natural Science Fund of China (Grant No. 50073001).

## References

1. Kudo, T.; Gordon, M. S. *J Am Chem Soc* 1998, 120, 11432.
2. Haddad, T. S.; Lichtenhan, J. D. *Macromolecules* 1996, 29, 7302.
3. Mater, P. T.; Jeon, H. G.; Romo-Urbe, A.; Haddad, T. S.; Lichtenhan, J. D. *Macromolecules* 1999, 32, 1194.
4. Xu, H.; Kuo, S. W.; Lee, J. S.; Chang, F. C. *Macromolecules* 2002, 35, 8788.
5. Mantz, R. A.; Jones, P. F.; Chaffee, K. P.; Lichtenhan, J. D.; Gilman, J. W.; Ismail, I. B. M.; Burmeister, M. *J Chem Mater* 1996, 8, 1250.
6. Zheng, L.; Farris, R. J.; Coughlin, E. B. *Macromolecules* 2001, 34, 8034.
7. Lichtenhan, J. D.; Otonari, Y. A.; Carr, M. J. *Macromolecules* 1995, 28, 8435.
8. Tschucida, A.; Bolln, C.; Sernetz, F.; Frey, H.; Mulhaupt, R. *Macromolecules* 1997, 30, 2818.
9. Lichtenhan, J. D.; Vu, Q. N.; Cater, J. A.; Gilman, J. W.; Feher, F. *Macromolecules* 1993, 26, 2141.
10. Lee, A.; Lichtenhan, J. D. *Macromolecules* 1998, 31, 4970.
11. Tang, B. Z.; Xu, H.; Lam, J. W. Y.; Lee, P. P. S.; Xu, K.; Sun, Q.; Cheuk, K. L. *Chem Mater* 2000, 12, 1446.
12. Auner, N.; Bats, J. W.; Katsoulis, D. E.; Suto, M.; Techlenburg, R. E.; Zank, G. A. *Chem Mater* 2000, 12, 3402.
13. Bharadwag, R. K.; Berry, R. J.; Farmer, B. L. *Polymer* 2000, 41, 7209.
14. Pyun, J.; Matyjaszewski, K. *Macromolecules* 2000, 33, 217.
15. Zheng, L.; Kasi, R. M.; Farris, R. J.; Coughlin, E. B. *J Polym Sci Part A: Polym Chem* 2002, 40, 885.
16. Marcolli, C.; Calzaferri, G. *Appl Organomet Chem* 1999, 13, 213.
17. Wallace, W. E.; Guttman, C. M.; Antonucci, J. M. *Polymer* 2000, 41, 2219.